

## Theory of Anisotropic Exchange in Laterally Coupled Quantum Dots

Fabio Baruffa,<sup>1</sup> Peter Stano,<sup>2,3</sup> and Jaroslav Fabian<sup>1</sup>

<sup>1</sup>*Institute for Theoretical Physics, University of Regensburg, 93040 Regensburg, Germany*

<sup>2</sup>*Institute of Physics, Slovak Academy of Sciences, 84511 Bratislava, Slovak Republic*

<sup>3</sup>*Physics Department, University of Arizona, 1118 East 4th Street, Tucson, Arizona 85721, USA*

(Received 20 August 2009; published 23 March 2010)

The effects of spin-orbit coupling on the two-electron spectra in lateral coupled quantum dots are investigated analytically and numerically. It is demonstrated that in the absence of magnetic field, the exchange interaction is practically unaffected by spin-orbit coupling, for any interdot coupling, boosting prospects for spin-based quantum computing. The anisotropic exchange appears at finite magnetic fields. A numerically accurate effective spin Hamiltonian for modeling spin-orbit-induced two-electron spin dynamics in the presence of magnetic field is proposed.

DOI: 10.1103/PhysRevLett.104.126401

PACS numbers: 71.70.Gm, 71.70.Ej, 73.21.La, 75.30.Et

The electron spins in quantum dots are natural and viable qubits for quantum computing [1], as evidenced by the impressive recent experimental progress [2,3] in spin detection and spin relaxation [4,5], as well as in coherent spin manipulation [6,7]. In coupled dots, the two-qubit quantum gates are realized by manipulating the exchange coupling which originates in the Coulomb interaction and the Pauli principle [1,8]. How is the exchange modified by the presence of the spin-orbit coupling? In general, the usual (isotropic) exchange changes its magnitude while a new, functionally different form of exchange, called anisotropic, appears, breaking the spin-rotational symmetry. Such changes are a nuisance from the perspective of the error correction [9], although the anisotropic exchange could also induce quantum gating [10,11].

The anisotropic exchange of coupled localized electrons has a convoluted history [12–18]. The question boils down to determining the leading order in which the spin-orbit coupling affects both the isotropic and anisotropic exchange. At zero magnetic field, the second order was suggested [19], with later revisions showing the effects are absent in the second order [12,20].

Here, we perform numerically exact calculations of the isotropic and anisotropic exchange in realistic GaAs coupled quantum dots in the presence of both the Dresselhaus and Bychkov-Rashba spin-orbit interactions [21]. We establish that in zero magnetic field, the second-order spin-orbit effects are absent at *all* interdot couplings. Neither is the isotropic exchange affected, nor is the anisotropic exchange present. At finite magnetic fields, the anisotropic coupling appears. We derive a spin-exchange Hamiltonian describing this behavior, generalizing the existing descriptions; we do not rely on weak coupling approximations such as the Heitler-London one. The model is proven highly accurate by comparison with our numerics, and we propose it as a realistic effective model for the two-spin dynamics in coupled quantum dots.

Our microscopic description is the single band effective mass envelope function approximation; we neglect multi-

band effects [22,23]. We consider a two-electron double dot whose lateral confinement is defined electrostatically by metallic gates on the top of a semiconductor heterostructure. The heterostructure, grown along the [001] direction, provides strong perpendicular confinement, such that electrons are strictly two-dimensional, with the Hamiltonian (subscript  $i$  labels the electrons)

$$H = \sum_{i=1,2} (T_i + V_i + H_{Z,i} + H_{so,i}) + H_C. \quad (1)$$

The single-electron terms are the kinetic energy, model confinement potential, and the Zeeman term,

$$T = \mathbf{P}^2/2m = (-i\hbar\nabla + e\mathbf{A})^2/2m, \quad (2)$$

$$V = (1/2)m\omega^2[\min\{(x-d)^2, (x+d)^2\} + y^2], \quad (3)$$

$$H_Z = (g/2)(e\hbar/2m_e)\mathbf{B} \cdot \boldsymbol{\sigma} = \mu\mathbf{B} \cdot \boldsymbol{\sigma}, \quad (4)$$

and spin-orbit interactions—linear and cubic Dresselhaus, and Bychkov-Rashba [21],

$$H_d = (\hbar/ml_d)(-\sigma_x P_x + \sigma_y P_y), \quad (5)$$

$$H_{d3} = (\gamma_c/2\hbar^3)(\sigma_x P_x P_y^2 - \sigma_y P_y P_x^2) + \text{Herm.conj.}, \quad (6)$$

$$H_{br} = (\hbar/ml_{br})(\sigma_x P_y - \sigma_y P_x), \quad (7)$$

which we lump together as  $H_{so} = \mathbf{w} \cdot \boldsymbol{\sigma}$ . The position  $\mathbf{r}$  and momentum  $\mathbf{P}$  vectors are two dimensional (in-plane);  $m/m_e$  is the effective/electron mass,  $e$  is the proton charge,  $\mathbf{A} = B_z(-y, x)/2$  is the in-plane vector potential to magnetic field  $\mathbf{B} = (B_x, B_y, B_z)$ ,  $g$  is the electron  $g$  factor,  $\boldsymbol{\sigma}$  are Pauli matrices, and  $\mu$  is the renormalized magnetic moment. The double dot confinement is modeled by two equal single dots displaced along [100] by  $\pm d$ , each with a harmonic potential with confinement energy  $\hbar\omega$ . The spin-orbit interactions are parametrized by the bulk material constant  $\gamma_c$  and the heterostructure dependent spin-orbit

lengths  $l_{br}$ ,  $l_d$ . Finally, the Coulomb interaction is  $H_C = (e^2/4\pi\epsilon)|\mathbf{r}_1 - \mathbf{r}_2|^{-1}$ , with the dielectric constant  $\epsilon$ .

The numerical results are obtained by exact diagonalization (configuration interaction method). The two-electron Hamiltonian is diagonalized in the basis of Slater determinants constructed from numerical single-electron states in the double dot potential. Typically, we use 21 single-electron states, resulting in the relative error for energies of order  $10^{-5}$ . We use material parameters of GaAs:  $m = 0.067m_e$ ,  $g = -0.44$ ,  $\gamma_c = 27.5$  meV  $\text{\AA}^3$ , a single dot confinement energy  $\hbar\omega = 1.1$  meV, and spin-orbit lengths  $l_d = 1.26$   $\mu\text{m}$  and  $l_{br} = 1.72$   $\mu\text{m}$  from a fit to a spin relaxation experiment [24,25].

Let us first neglect the spin and look at the spectrum in zero magnetic field as a function of the interdot distance ( $2d$ ) and tunneling energy, Fig. 1. At  $d = 0$ , our model describes a single dot. The interdot coupling gets weaker as one moves to the right; both the isotropic exchange  $J$  and the tunneling energy  $T$  decay exponentially. The symmetry of the confinement potential assures the electron wave functions are symmetric or antisymmetric upon inversion. The two lowest states,  $\Psi_{\pm}$ , are separated from the higher excited states by an appreciable gap  $\Delta$ , what justifies the restriction to the two lowest orbitals for the spin qubit pair at a weak coupling. Further derivations are based on

$$P\Psi_{\pm} = \pm\Psi_{\pm}, \quad I_1I_2\Psi_{\pm} = \pm\Psi_{\pm}, \quad (8)$$

where  $If(x, y) = f(-x, -y)$  is the inversion operator and  $Pf_1g_2 = f_2g_1$  is the particle exchange operator. Functions  $\Psi_{\pm}$  in the Heitler-London approximation fulfill Eq. (8). However, unlike Heitler-London, Eq. (8) is valid generally

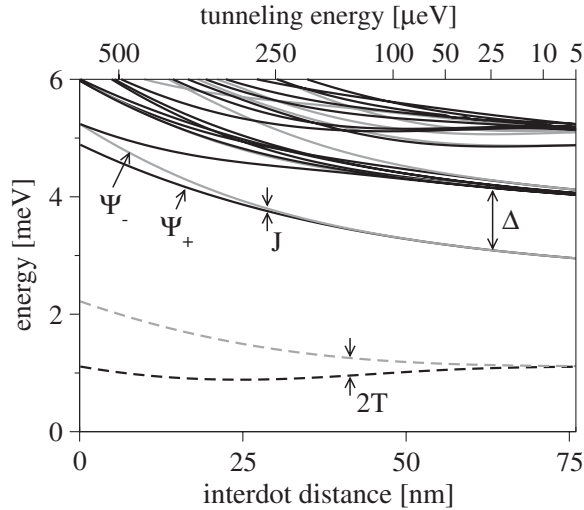


FIG. 1. Calculated double dot spectrum as a function of the interdot distance and tunneling energy. Spin is not considered, and the magnetic field is zero. Solid lines show the two-electron energies. The two lowest states are explicitly labeled, split by the isotropic exchange  $J$  and displaced from the nearest higher excited state by  $\Delta$ . For comparison, the two lowest single-electron states are shown (dashed lines), split by twice the tunneling energy  $T$ . State spatial symmetry is denoted by darker (symmetric) and lighter (antisymmetric) lines.

in symmetric double dots, as we learn from numerics (we saw it valid in all cases we studied).

Let us reinstate the spin. The restricted two-qubit subspace amounts to the following four states ( $S$  stands for singlet,  $T$  for triplet),

$$\{\Phi_i\}_{i=1,\dots,4} = \{\Psi_+S, \Psi_-T_+, \Psi_-T_0, \Psi_-T_-\}. \quad (9)$$

Within this basis, the system is described by a 4 by 4 Hamiltonian with matrix elements  $(H_4)_{ij} = \langle\Phi_i|H|\Phi_j\rangle$ . Without spin-orbit interactions, this Hamiltonian is diagonal, with the singlet and triplets split by the isotropic exchange  $J$  [1,8], and the polarized triplets Zeeman split. It is customary to refer only to the spinor part of the basis states resulting in the isotropic exchange Hamiltonian,

$$H_{iso} = (J/4)\boldsymbol{\sigma}_1 \cdot \boldsymbol{\sigma}_2 + \mu\mathbf{B} \cdot (\boldsymbol{\sigma}_1 + \boldsymbol{\sigma}_2). \quad (10)$$

A naive approach to include the spin-orbit interaction is to consider it within the basis of Eq. (9). This gives the Hamiltonian  $H'_{ex} = H_{iso} + H'_{aniso}$ , where

$$H'_{aniso} = \mathbf{a}' \cdot (\boldsymbol{\sigma}_1 - \boldsymbol{\sigma}_2) + \mathbf{b}' \cdot (\boldsymbol{\sigma}_1 \times \boldsymbol{\sigma}_2), \quad (11)$$

with the six real parameters given by spin-orbit vectors

$$\mathbf{a}' = \text{Re}\langle\Psi_+|\mathbf{w}_1|\Psi_-\rangle, \quad \mathbf{b}' = \text{Im}\langle\Psi_+|\mathbf{w}_1|\Psi_-\rangle. \quad (12)$$

The form of the Hamiltonian follows solely from the inversion symmetry  $I\mathbf{w} = -\mathbf{w}$  and Eq. (8). The spin-orbit coupling appears in the first order.

The Hamiltonian  $H'_{ex}$  fares badly with numerics. Figure 2 shows the energy shifts caused by the spin-orbit coupling for selected states, at different interdot couplings and perpendicular magnetic fields. The model is completely off even though we use numerical wave functions  $\Psi_{\pm}$  in Eq. (12) without further approximations.

To proceed, we remove the linear spin-orbit terms from the Hamiltonian using transformation [20,26,27]

$$U = \exp[-(i/2)\mathbf{n}_1 \cdot \boldsymbol{\sigma}_1 - (i/2)\mathbf{n}_2 \cdot \boldsymbol{\sigma}_2], \quad (13)$$

where  $\mathbf{n} = (x/l_d - y/l_{br}, x/l_{br} - y/l_d, 0)$ .

Up to the second order in small quantities (the spin-orbit and Zeeman interactions), the transformed Hamiltonian  $\tilde{H} = UH_4U^\dagger$  is the same as the original, Eq. (1), except for the linear spin-orbit interactions:

$$\tilde{H}_{so} = -(\mu\mathbf{B} \times \mathbf{n}) \cdot \boldsymbol{\sigma} + (K_-/\hbar)L_z\sigma_z - K_+, \quad (14)$$

where  $K_{\pm} = (\hbar^2/4ml_d^2) \pm (\hbar^2/4ml_{br}^2)$ . In the unitarily transformed basis, we again restrict the Hilbert space to the lowest four states, getting the effective Hamiltonian

$$H_{ex} = (J/4)\boldsymbol{\sigma}_1 \cdot \boldsymbol{\sigma}_2 + \mu(\mathbf{B} + \mathbf{B}_{so}) \cdot (\boldsymbol{\sigma}_1 + \boldsymbol{\sigma}_2) + \mathbf{a} \cdot (\boldsymbol{\sigma}_1 - \boldsymbol{\sigma}_2) + \mathbf{b} \cdot (\boldsymbol{\sigma}_1 \times \boldsymbol{\sigma}_2) - 2K_+. \quad (15)$$

The operational form is the same as for  $H'_{ex}$ . The qualitative difference is in the way the spin-orbit enters the parameters. First, an effective Zeeman term appears,

$$\mu\mathbf{B}_{so} = \hat{\mathbf{z}}(K_-/\hbar)\langle\Psi_-|L_{z,1}|\Psi_-\rangle. \quad (16)$$

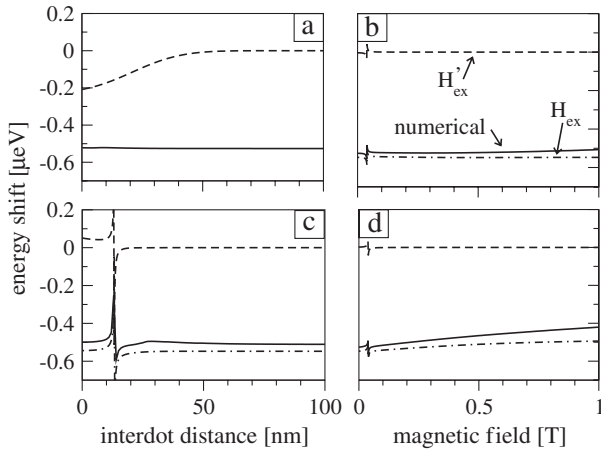


FIG. 2. The spin-orbit induced energy shift as a function of the interdot distance (left) and perpendicular magnetic field (right). (a) Singlet in zero magnetic field, (c) singlet at 1 Tesla field, (b) and (d) singlet and triplet  $T_+$  at the interdot distance 55 nm corresponding to the zero-field isotropic exchange of  $1 \mu\text{eV}$ . The exchange models  $H'_{\text{ex}}$  (dashed line) and  $H_{\text{ex}}$  (dot-dashed line) are compared with the numerics (solid line).

Second, the spin-orbit vectors are linearly proportional to both the spin-orbit coupling and magnetic field,

$$\mathbf{a} = -\mu\mathbf{B} \times \text{Re}\langle\Psi_+|\mathbf{n}_1|\Psi_-\rangle, \quad (17a)$$

$$\mathbf{b} = -\mu\mathbf{B} \times \text{Im}\langle\Psi_+|\mathbf{n}_1|\Psi_-\rangle. \quad (17b)$$

The effective model and the exact data agree very well for all interdot couplings, as seen in Fig. 2.

At zero magnetic field, only the first and the last term in Eq. (15) survive. This is the result of Ref. [20], where primed operators were used to refer to the fact that the Hamiltonian  $H_{\text{ex}}$  refers to the transformed basis,  $\{U\Phi_i\}$ . Note that if a basis separable in orbital and spin part is required, undoing  $U$  necessarily yields the original Hamiltonian Eq. (1), and the restriction to the four lowest states gives  $H'_{\text{ex}}$ . Replacing the coordinates  $(x, y)$  by mean values  $(\pm d, 0)$  [12] visualizes the Hamiltonian  $H_{\text{ex}}$  as an interaction through rotated sigma matrices, but this is just an approximation, valid if  $d, l_{\text{so}} \gg l_0$ .

One of our main numerical results is establishing the validity of the Hamiltonian in Eq. (15) for  $B = 0$ , confirming recent analytic predictions and extending their applicability beyond the weak coupling limit. In the transformed basis, the spin-orbit interactions do not lead to any anisotropic exchange, nor do they modify the isotropic one. In fact, this result could have been anticipated from its single-electron analog: at zero magnetic field, there is no spin-orbit contribution to the tunneling energy [28], going opposite to the intuitive notion of the spin-orbit coupling induced coherent spin rotation and spin-flip tunneling amplitudes. Figure 3(a) summarizes this case: the isotropic exchange is the only nonzero parameter in  $H_{\text{ex}}$ , while there is a finite anisotropic exchange in  $H'_{\text{ex}}$  [29].

From the concept of dressed qubits [30], it follows that the main consequence of the spin-orbit interaction, the basis transformation  $U$ , is not a nuisance for quantum computation. We expect the same holds for a qubit array, since the electrons are at fixed positions and a long distance tunneling is not possible. However, a rigorous analysis of this point is beyond the scope of this Letter. If electrons are allowed to move,  $U$  results in the spin relaxation [31].

Figure 3(b) shows model parameters in 1 Tesla perpendicular magnetic field. The isotropic exchange again decays exponentially. As it becomes smaller than the Zeeman energy, the singlet state anticrosses one of the polarized triplets (seen as cusps on Fig. 2). Here, it is  $T_+$ , as both the isotropic exchange and the  $g$  factor are negative. Because the Zeeman energy dominates the spin-dependent terms and the singlet and triplet  $T_0$  are not coupled (see below), the anisotropic exchange influences the energy in the second-order [12]. Note the difference in the strengths. In  $H'_{\text{ex}}$ , the anisotropic exchange falls off exponentially, while  $H_{\text{ex}}$  predicts nonexponential behavior, resulting in spin-orbit effects larger by orders of magnitude. The effective magnetic field  $B_{\text{so}}$  is always much smaller than the real magnetic field and can be neglected in most cases.

Figure 3(c) compares analytical models. In zero field and no spin-orbit interactions, the isotropic exchange Hamiltonian  $H_{\text{iso}}$  describes the system. Including the spin-orbit coupling in the first order,  $H'_{\text{ex}}$ , gives a nonzero coupling between the singlet and triplet  $T_0$ . Going to the

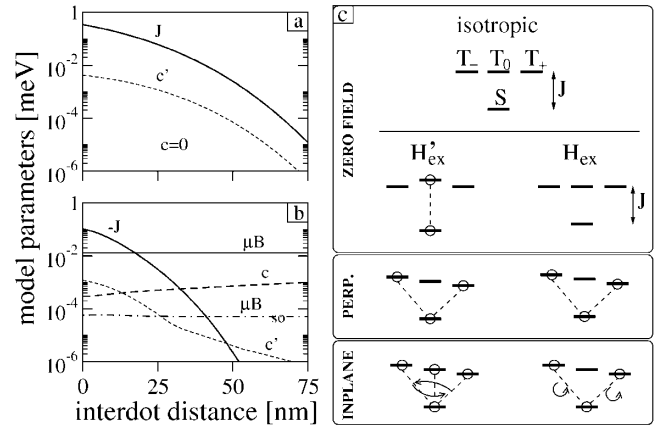


FIG. 3. (a) The isotropic and anisotropic exchange as functions of the interdot distance at zero magnetic field. (b) The isotropic exchange  $J$ , anisotropic exchange  $c/c'$ , the Zeeman splitting  $\mu B$ , and its spin-orbit part  $\mu B_{\text{so}}$  at perpendicular magnetic field of 1 T. (c) Schematics of the exchange-split four lowest states for the three models,  $H_{\text{iso}}$ ,  $H'_{\text{ex}}$ , and  $H_{\text{ex}}$ , which include the spin-orbit coupling in no, first, and second order, respectively, at zero magnetic field (top). The latter two models are compared in perpendicular and in-plane magnetic fields as well. The eigenenergies are indicated by the solid lines. The dashed lines show which states are coupled by the spin-orbit coupling. The arrows indicate the redistribution of the couplings as the in-plane field direction changes with respect to the crystallographic axes (see the main text).



second order, the effective model  $H_{\text{ex}}$  shows there are no spin-orbit effects (other than the basis redefinition).

The Zeeman interaction splits the three triplets in a finite magnetic field. Both  $H'_{\text{ex}}$  and  $H_{\text{ex}}$  predict the same type of coupling in a perpendicular field, between the singlet and the two polarized triplets. Interestingly, in in-plane fields, the two models differ qualitatively. In  $H'_{\text{ex}}$  the spin-orbit vectors are fixed in the plane. Rotation of the magnetic field “redistributes” the couplings among the triplets. (This anisotropy is due to the  $C_{2v}$  symmetry of the two-dimensional electron gas in GaAs, imprinted in the spin-orbit interactions [21].) In contrast, the spin-orbit vectors of  $H_{\text{ex}}$  are always perpendicular to the magnetic field. Remarkably, aligning the magnetic field along a special direction (here, we allow an arbitrary positioned dot, with  $\delta$  the angle between the main dot axis and the crystallographic  $x$  axis),

$$[(l_{\text{br}} - l_d \tan \delta)(l_d - l_{\text{br}} \tan \delta)0], \quad (18)$$

all the spin-orbit effects disappear once again, as if  $B$  were zero. (An analogous angle was reported for a single dot in Ref. [32]). This has strong implications for the spin-orbit induced singlet-triplet relaxation [33–36]. Indeed,  $S \leftrightarrow T_0$  transitions are ineffective at any magnetic field, as these two states are never coupled in  $H_{\text{ex}}$  model. Second,  $S \leftrightarrow T_{\pm}$  transitions will show strong (orders of magnitude) anisotropy with respect to the field direction, with minimum along the vector in Eq. (18). This prediction is directly testable in experiments on two-electron spin relaxation.

Our derivation was based on the inversion symmetry of the potential only. What are the limits of our model? We neglected third order terms in  $\tilde{H}_{\text{so}}$  and, restricting the Hilbert space, corrections from higher excited orbital states. (Among the latter is the nonexponential spin-spin coupling [12]). Compared to the second-order terms we keep, these are smaller by (at least)  $d/l_{\text{so}}$  and  $c/\Delta$ , respectively [33]. Apart from the analytical estimates, the numerics, which includes all terms, assures us that both of these are negligible. Based on numerics, we also conclude our analytical model stays quantitatively faithful even at the strong coupling limit, where  $\Delta \rightarrow 0$ . More involved is the influence of the cubic Dresselhaus term, which is not removed by the unitary transformation. This term is the main source for the discrepancy of the model and the numerical data in finite fields. Most importantly, it does not change our results for  $B = 0$ .

Concluding, we studied the effects of spin-orbit coupling on the exchange in lateral coupled GaAs quantum dots. We derive and support by precise numerics an effective Hamiltonian for two-spin qubits, generalizing the existing models. The effective anisotropic exchange model should be useful in precise analysis of the physical realizations of quantum computing schemes based on quantum dot spin qubits, as well as in the physics of electron spins in quantum dots in general.

This work was supported by DFG GRK 638, SPP 1285, NSF Grant Nos. DMR-0706319, RPEU-0014-06, ERDF OP R and D “QUTE,” CE SAS QUTE and DAAD.

- 
- [1] D. Loss and D.P. DiVincenzo, Phys. Rev. A **57**, 120 (1998).
  - [2] R. Hanson *et al.*, Rev. Mod. Phys. **79**, 1217 (2007).
  - [3] J. M. Taylor *et al.*, Phys. Rev. B **76**, 035315 (2007).
  - [4] J. M. Elzerman *et al.*, Nature (London) **430**, 431 (2004).
  - [5] F. H. L. Koppens *et al.*, Phys. Rev. Lett. **100**, 236802 (2008).
  - [6] J. R. Petta *et al.*, Science **309**, 2180 (2005).
  - [7] K. C. Nowack *et al.*, Science **318**, 1430 (2007).
  - [8] X. Hu and S. Das Sarma, Phys. Rev. A **61**, 062301 (2000).
  - [9] D. Stepanenko *et al.*, Phys. Rev. B **68**, 115306 (2003).
  - [10] D. Stepanenko and N. E. Bonesteel, Phys. Rev. Lett. **93**, 140501 (2004).
  - [11] N. Zhao *et al.*, Phys. Rev. B **74**, 075307 (2006).
  - [12] S. Gangadharaiah, J. Sun, and O. A. Starykh, Phys. Rev. Lett. **100**, 156402 (2008).
  - [13] L. Shekhtman, O. Entin-Wohlman, and A. Aharony, Phys. Rev. Lett. **69**, 836 (1992).
  - [14] A. Zheludev *et al.*, Phys. Rev. B **59**, 11432 (1999).
  - [15] Y. Tserkovnyak and M. Kindermann, Phys. Rev. Lett. **102**, 126801 (2009).
  - [16] S. Chutia, M. Friesen, and R. Joynt, Phys. Rev. B **73**, 241304(R) (2006).
  - [17] L. P. Gorkov and P. L. Krotkov, Phys. Rev. B **67**, 033203 (2003).
  - [18] S. D. Kunikeev and D. A. Lidar, Phys. Rev. B **77**, 045320 (2008).
  - [19] K. V. Kavokin, Phys. Rev. B **64**, 075305 (2001).
  - [20] K. V. Kavokin, Phys. Rev. B **69**, 075302 (2004).
  - [21] J. Fabian *et al.*, Acta Phys. Slovaca **57**, 565 (2007).
  - [22] S. C. Badescu, Y. B. Lyanda-Geller, and T. L. Reinecke, Phys. Rev. B **72**, 161304(R) (2005).
  - [23] M. M. Glazov and V. D. Kulakovskii, Phys. Rev. B **79**, 195305 (2009).
  - [24] P. Stano and J. Fabian, Phys. Rev. Lett. **96**, 186602 (2006).
  - [25] P. Stano and J. Fabian, Phys. Rev. B **74**, 045320 (2006).
  - [26] I. L. Aleiner and V. I. Fal'ko, Phys. Rev. Lett. **87**, 256801 (2001).
  - [27] L. S. Levitov and E. I. Rashba, Phys. Rev. B **67**, 115324 (2003).
  - [28] P. Stano and J. Fabian, Phys. Rev. B **72**, 155410 (2005).
  - [29] The spin-orbit vectors are determined up to the relative phase of states  $\Psi_+$  and  $\Psi_-$ . The observable quantity is  $c = \sqrt{a^2 + b^2}$  and analogously for  $c' = \sqrt{a'^2 + b'^2}$ .
  - [30] L.-A. Wu and D. A. Lidar, Phys. Rev. Lett. **91**, 097904 (2003).
  - [31] K. V. Kavokin, Semicond. Sci. Technol. **23**, 114009 (2008).
  - [32] V. N. Golovach, A. Khaetskii, and D. Loss, Phys. Rev. B **77**, 045328 (2008).
  - [33] O. Olendski and T. V. Shahbazyan, Phys. Rev. B **75**, 041306(R) (2007).
  - [34] K. Shen and M. W. Wu, Phys. Rev. B **76**, 235313 (2007).
  - [35] E. Y. Sherman and D. J. Lockwood, Phys. Rev. B **72**, 125340 (2005).
  - [36] J. I. Climente *et al.*, Phys. Rev. B **75**, 081303(R) (2007).